

# An Application of Range-Frequency Striations to Seafloor Inversion in Shallow Oceans

Adrian D. Jones, David W. Bartel and Paul A. Clarke

Defence Science and Technology Organisation, P.O. Box 1500, Edinburgh, SA 5111, Australia

## ABSTRACT

For shallow oceans, as is well known, multi-path interference generates a pattern of striations when broadband data received from a source are viewed on a range-frequency display. The frequency variations within this data are known to be related to the ocean depth, and to the seafloor acoustic properties (Jones and Clarke, Proceedings of 20th Intl. Congress on Acoustics, ICA 2010). Using a process in which the frequency spacing of the data is extracted, it is shown that a reasonable description of the seafloor acoustic properties may be inverted from the striations. The technique is demonstrated by simulations for a seafloor consisting of a uniform half-space.

## INTRODUCTION

It is well known that sound transmission in shallow oceans is critically dependent upon the features of the underwater environment. At low acoustic frequencies (less than about 300 Hz), or with a sound speed versus depth function which causes downward refraction, transmission to long range (30 km or more) is affected significantly by the seafloor reflective properties. At short to medium ranges (up to about 5 km) the acoustic reflectivity of the seafloor is significant for all frequencies. It is thus important that the acoustic reflectivity of the seafloor be known if descriptions of sound transmission are required.

For the short to medium ranges mentioned above, it is well known that the multiple paths of acoustic transmission combine constructively and destructively such that sound transmitted over a broad frequency band forms a pattern of lines, known as “striations”, when amplitude levels at each range are plotted against frequency. An example of such a plot is shown in Figure 1 for a seafloor half-space of coarse sand.

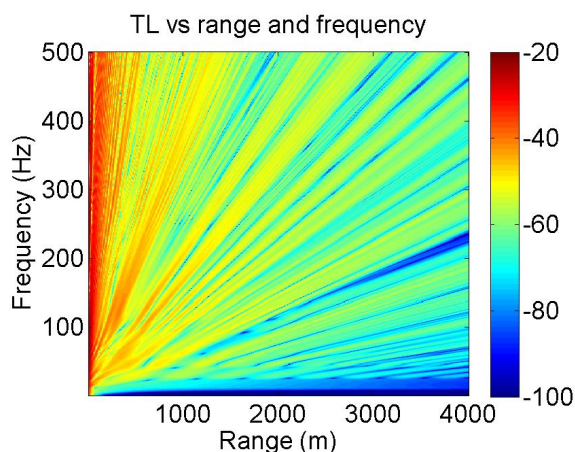


Figure 1. Simulated range-frequency  $TL$ , frequency to 500 Hz, for 80 m ocean, coarse sand seafloor

Figure 1 shows a simulation of Transmission Loss ( $TL$ ) for source to receiver horizontal range values at 10 m steps to 4000 m and for source frequencies at 1 Hz steps to 500 Hz. The wavenumber-integral model HANKEL (Bartel 2010)

was used for these simulations. The ocean is isovelocity (1500 m/s), depth 80 m, with both source and receiver at 18 m depth. The geoacoustic parameters describing the coarse sand are taken from Jensen and Kuperman's (1983) Table 1. Key values are the compressional speed 1800 m/s and shear speed 600 m/s.

The data in Figure 1 are values of  $TL$ , but may be considered as values of received signal level. In fact, if the Source Level at a 1 metre distance is 0.0 dB, and the source is omnidirectional, the values are equivalent. The data displayed in Figure 1 are dependent on the features of the environment which affect the transmission multi-paths, such as the amplitude and phase angle of reflections from the seafloor. The nature of the range-frequency striations is thus encoded with the seafloor characteristics. In recent years, there has been much interest in inverting the striations data to obtain seafloor properties (e.g. Heaney 2004). In the main, existing techniques have involved obtaining a best-fit of a set of proposed geoacoustic parameters to the striations data. This paper describes a new technique based on direct processing of the received data.

## RANGE-FREQUENCY STRIATIONS

The occurrence of range-frequency striations in received broadband data may be understood by examining the nature of phase coherent addition of multi-path arrivals. This is explained briefly, below.

Consider a single pair of arrivals at a receiver at any given depth, at horizontal range  $r$  from a source emitting a signal at frequency  $f$ . Consider that these arrivals are in phase at range  $r$  and frequency  $f$ . Clearly, if one of either frequency or range is changed, a phase difference will exist between the arrivals. If, for example, range is changed by  $\Delta r$ , it is obvious that a suitably chosen change in frequency  $\Delta f$  will result in the two arrivals maintaining an in-phase relationship. On a range-frequency plot there will then be the appearance of a line or band of in-phase data in accord with some function of  $r$  and  $f$ . The nature of the function  $\Delta r/\Delta f$  that maintains the phase relationship along the lines, or “striations”, may be understood by considerations of ray acoustics in an isovelocity ocean, as shown in Figure 2.

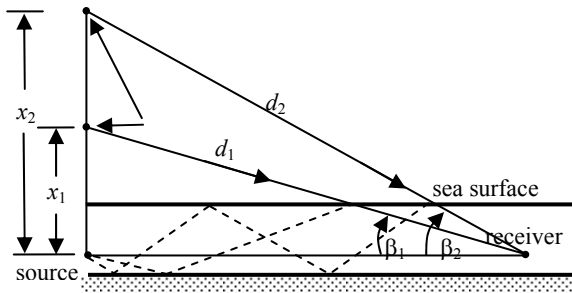


**Figure 2.** Simulated range-frequency  $TL$ , for 50 m ocean

In the general case of an isovelocity ocean, the difference in phase, due to path length differences, between particular arrivals may be shown to be  $\frac{2\pi f}{c_w} [d_2 - d_1]$  radians, where  $d_2$

and  $d_1$  are source to receiver path lengths for rays #1 and #2 and  $c_w$  is the speed of sound in seawater. Thus, it follows that the rate of change of phase between these arrivals, as a function of frequency  $f$ , is exactly given by

$$\frac{d\phi}{df} = \frac{2\pi}{c_w} [d_2 - d_1] \text{ radians/Hz.} \quad (1)$$

The rate of change of phase between these arrivals, as a function of range  $r$ , due to path length changes, may likewise be determined. Here, the assumption that grazing angles are small (e.g. in accord with  $n \ll (r/2D)$ ) where  $D$  is ocean depth and  $n$  is the number of seafloor reflections, being the same as the order number in a ray family) permits the approximate expression:

$$\frac{d\phi}{dr} = \frac{2\pi f}{c_w} \left[ \frac{d_1 - d_2}{r} \right] \text{ radians/metre.} \quad (2)$$

It is clear from Equations (1) and (2) that a phase change between the ray arrivals due to a change in frequency is equivalent to a phase change between the same arrivals due to a change in source to receiver range, with a constant of proportionality which varies linearly in frequency and inversely in range. An important consequence is that the phase relationship between two arrivals may be held at zero if the frequency is increased by  $\Delta f$  and the range increased by  $(r \Delta f)/f$ . A consequence is that  $\Delta f/\Delta r = f/r$  along the region of unchanged phase separation, and so lines, referenced here as striations, appear on the range-frequency plot. Further, if the range and frequency axes are linear, then the striations will appear on the plot as straight lines originating from the origin, as is obvious from Figure 1.

The above analysis includes a number of assumptions. Firstly, the model of transmission must permit a continuous variation of grazing angles  $\beta_1$  and  $\beta_2$ . If there is an insufficient number of propagating modes, the simple analysis used above will be invalid. Secondly, the rate of change of the phase difference with range  $\frac{d\phi}{dr}$  must be dominated by the

path length effects described by Equation (2). It must be remembered that the reflection at the seafloor includes a phase angle change, and that this is dependent on grazing angle, and so for a particular multi-path is then dependent on range. Although not shown here, it may be determined that

the phase change due to ‘‘range effect’’, as described by Equation (2), dominates the phase change due to ‘‘seafloor effect’’ so long as

$$f > \frac{m n c_w}{2\pi D \sqrt{1 - n_r^2}} \text{ Hz} \quad (3)$$

where  $m$  is the ratio of seafloor density to seawater density,  $n$  is the order number in the ray family for the particular multi-path, and  $n_r$  is the seawater to seafloor index of refraction. This is reliant upon a simplification of the well-known (e.g. see Brekhovskikh and Lysanov (2003) equation 3.1.15) re-

flection phase angle function  $\phi = -2 \arctan \left[ \frac{\sqrt{\cos^2 \beta - n_r^2}}{m \sin \beta} \right]$

for a fluid seafloor for angles less than the critical angle. For an ocean of 100 m depth, for typical values of  $m$  and  $n_r$ , at a frequency of 100 Hz the requirement is satisfied for arrivals up to at least order  $n \approx 10$ .

A more formal expression of the result from this simplified analysis is

$$\frac{r}{f} \frac{df}{dr} = 1, \text{ that is } \frac{r}{\omega} \frac{d\omega}{dr} = 1 \quad (4)$$

where  $\omega$  is angular frequency,  $2\pi f$ . As shown by, for example, Brekhovskikh and Lysanov (2003), section 6.7.2, the quantity  $\frac{r}{\omega} \frac{d\omega}{dr}$ , which is usually represented in the literature

as  $\beta$ , is an invariant for a waveguide, but is not necessarily of value 1.0. In fact, Brekhovskikh and Lysanov’s equation 6.7.39 shows that the invariant  $\beta$  is a function of the phase velocity and group velocity of the modes under consideration. They show that for a homogeneous ocean with a perfectly reflecting seafloor, for modes with small grazing angles at the surface and seafloor,  $\beta \approx 1$ .

The analysis described by Equations (1) and (2), and the situation shown in Figure 2, is applicable to Lloyd mirror interference (e.g. Urlick (1983) page 131) for which there are two transmission paths only: the direct path and the path with one surface reflection. The expression (4) is equally applicable, and so striations due to Lloyd mirror interference will appear to have the same slope on a range-frequency plot as do the striations due to multi-path interference.

### Spectral Variability

Although not immediately apparent from the data in Figure 1, it has been established (Jones and Clarke 2010, 2011) that the variation of signal amplitude with frequency, for an isovelocity shallow ocean, is independent of source to receiver range, for ranges values within certain bounds. It may appear from Figure 1 that the scale of frequency variability is increasing with range, however this is not the general case, notwithstanding the adherence of striations to the function  $\Delta f/\Delta r = f/r$ . For a given range, an average frequency spacing of the amplitude variation may be determined by the features of the environment as follows (Jones and Clarke 2010, 2011):

$$\Delta f_h \approx \frac{\ln(10)c_w F}{20\pi D} \text{ Hz} \approx 0.037 c_w F/D \text{ Hz} \quad (5)$$

where  $F$  dB/radian is the presumed function of bottom loss versus grazing angle,  $\Delta f_h$  is the frequency displacement in Hz at which the autocorrelation of received amplitude with frequency reduces to 0.5,  $D$  is ocean depth. Equation (5) was determined from considerations of the sound channel impulse response time, this also being independent of range so long as range assumptions described by Jones and Clarke (2011, 2010) are valid. The expression is based on an assumed intensity impulse response function of the form  $e^{-t/\tau}$ , which is applicable within certain limitations (Jones and Clarke 2010). An example of the bottom loss versus grazing angle function, showing the linear variation in dB at small grazing angles, is shown in Figure 3 for the coarse sand material used for Figure 1. The data contained in this figure have been processed to determine an average slope of bottom loss versus grazing angle from 0° to 10° of 9 dB/radian.

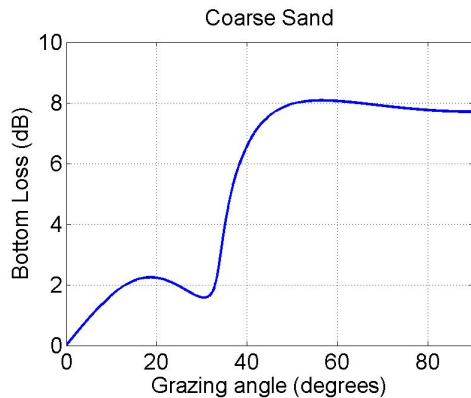


**Figure 3.** Bottom Loss versus grazing angle for coarse sand seafloor (parameters from Jensen & Kuperman (1983))

A consequence of Equation (5) is that the bottom loss versus grazing angle parameter  $F$  dB/radian may be inverted from broadband data received at a single range value, so long as range and frequency values are in accord with certain assumptions made in the analysis (Jones and Clarke 2010, 2011).

For highly multi-path environments, the fluctuations with frequency of the received sound pressure amplitude adhere to the Rayleigh distribution, approximately, as is well known. The frequency spacing between the maxima in these values is relevant to the present exercise. Schroeder (Schroeder and Kuttruff 1962, Schroeder 1987) considered this spacing for a multi-path transmission environment with Rayleigh distributed pressure amplitude values with an exponential impulse decay function. As the shallow water transmission channel is known to have an impulse decay function that approximates an exponential, Schroeder’s analysis is then relevant to the present case. Schroeder’s average spacing between maxima is  $7/T_{60}$  Hz, where  $T_{60}$  is the reverberation time, same as  $6\ln(10)\tau$ . This has the effect that the average spacing between maxima is about  $3\Delta f_h$  Hz, and may be assumed to apply to shallow water transmission.

### Spatial Variability

For a receiver at a given range and frequency, the changes in the amplitude of the sum of all multi-paths is related to the phase change that occurs between sets of arrivals due to ei-

ther a change in range or frequency. From the earlier analysis, the phase changes caused by a change in frequency  $\Delta f$ , are equivalent to the phase changes caused by a change in range  $-(r \Delta f)/f$ . It then follows that the spatial equivalent, in metres, to the average spacing of amplitude variation with frequency  $\Delta f_h$  is

$$\Delta x_{r,h} \approx \frac{\ln(10)rF\lambda}{20\pi D} \approx 0.037rF\lambda/D \text{ m} \quad (6)$$

where  $\Delta x_{r,h}$  is the spatial displacement in the radial direction, metres, at which the autocorrelation of received amplitude with range reduces to 0.5, and the substitution  $\lambda = c_w/f$  has been made. As for spectral variability, the summed multi-path values are Rayleigh distributed in amplitude about the mean, although the mean changes with range, of course. Equation (6) does not include the effects due to the changing mean. Again, as for the spectral variability case, the average range spacing between maxima may be roughly approximated as  $3\Delta x_{r,h}$  metres.

### Sound Source Issues

In many practical circumstances, the broadband signal generated by the source has no temporal coherence, and resembles random Gaussian noise. This will approximate the situation if the broadband signal is generated by a ship propeller, as is well known. For such a source, the received range-frequency plot no longer resembles that in Figure 1, which is based on phase-coherent transmission and zero ambient noise. With a ship as the signal source, the data on the range-frequency plot is obtained as a series of spectra received at subsequent times. Each of these spectra contains a value in each frequency bin which resembles a random sample about a mean determined by the multi-path combination. Each of these random samples is averaged according to the bandwidth-time product  $B \Delta t = n$  implied by temporal and spectral sampling. If there was a large degree of averaging of the signal received at every range step, the range-frequency plot *will* resemble the coherent result.

For a bandwidth-time product  $B \Delta t = n$  (i.e. averaging over  $n$  samples), the sample value in each frequency bin may be shown to be contained to a spread of  $\pm 2 \sigma$  about the true value, where

$$\sigma \approx \frac{4.3}{\sqrt{n}} \text{ dB} . \quad (7)$$

This result may be attributed to Tukey and Winsor, as shown by Blackman and Tukey (1959) in their Table II. For example, with bandwidth-time product of 10 the values in each of the frequency bins of the range-frequency plot are within  $\pm 2.7$  dB of the local mean value. Bearing in mind that the mean range-frequency values are Rayleigh distributed in each of range and frequency, with a standard deviation of dB values of 5.6 dB, averaging received ship-generated signals (e.g. with a bandwidth-time product of 10) will permit features of the true channel response to become evident. Figure 4 shows a simulation of the range-frequency data corresponding with Figure 1, but with the source waveform assumed to be a series of uncorrelated Gaussian values. In this case, the data are simulated for a bandwidth-time product of 1, that is, there

is no averaging. Clearly, the range-frequency plot in Figure 4 has the character of the data in Figure 1, however the detail is not as readily apparent.

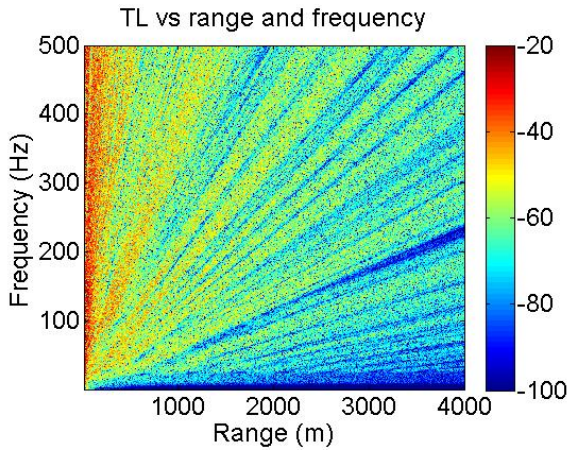


**Figure 4.** Simulated range-frequency received level, for 80 m ocean, coarse sand seafloor, uncorrelated Gaussian signal source,  $B\Delta t = 1$

Lastly, it must be noted that, with a vessel as the signal source, the receiver range changes over the duration of data collection. With a relative closing speed  $v$  m/s, the receipt of each spectrum may be equated with a range variation of  $v\Delta t$  metres, where  $\Delta t$  is the averaging time. Clearly, this distance must be less than the range  $\Delta x_{r,h}$  over which the interference field changes.

## INTERFERENCE FIELD-BASED INVERSION

The technique for inversion of seafloor reflectivity which is described in this paper is the spectral variability method of Jones and Clarke (2010, 2011). Here the features of the interference field which are implicit within the range-frequency data are used to obtain the value  $F$  dB/radian, the presumed function of bottom loss versus grazing angle. This, in turn, is inverted from Equation (5) as

$$F \approx \frac{27.3D\Delta f_h}{c_w} \text{ dB/radian.} \quad (8)$$

where  $\Delta f_h$ , the frequency displacement at which the autocorrelation of received amplitude with frequency reduces to 0.5, is obtained from spectral data. In practice, the data values within a single spectrum are processed to obtain a normalised autocorrelation of the amplitude of the sound channel frequency response,  $\rho_{|p|}(\Delta f)$ , and the frequency spacing at which the autocorrelation drops to 0.5 is read off. After Schroeder (1962), the normalised autocorrelation is carried out as

$$\rho_{|p|}(\Delta f) = \frac{\langle |p(f)||p(f+\Delta f)| \rangle - \langle |p(f)| \rangle^2}{\langle |p(f)|^2 \rangle - \langle |p(f)| \rangle^2} \quad (9)$$

where the autocorrelation is carried out on the zero-mean sound pressure modulus, that is, on  $|p(f)| - \langle |p(f)| \rangle$ .

If the source data for this autocorrelation are contained in a spectrum at a single range value from un-averaged data as in Figure 4, it is clear that use of Equation (9) may provide an unreliable estimate. Clearly, some averaging is desired to ensure that the spectrum values which are available for processing using Equation (9) are closer to the mean values.

## Data Averaging

The data in a given frequency bin may be averaged as a function of range, so that the averaged result may more closely approach the true local mean value. Here, the reduction in the spread of the estimate from the true mean is achieved at a rate dependent on the number of averages as described by Equation (7). A limit to which this range averaging may be achieved is indicated by the value  $\Delta x_{r,h}$  shown by Equation (6), as this describes an average change in range over which the true received amplitude value changes. At a range 3000 m from a source in an ocean of depth 80 m, at 200 Hz,  $\Delta x_{r,h} \approx 10.4F$  metres. Typically, the value of  $F$  may range from 5 dB/radian for a highly reflective seafloor to 80 dB/radian for a highly absorptive seafloor, such that  $\Delta x_{r,h}$  will be as small as about 50 metres or as large as about 800 m. The value of  $F$  for coarse sand, determined over the grazing angles  $0^\circ$  to  $10^\circ$ , is 9 dB/radian, with the result that the limit for simple range averaging for data at 200 Hz,  $\Delta x_{r,h} \approx 110$  metres. This is consistent with the data shown in Figure 1.

As the range-frequency striations are known to define persistent features within the spectral data, due to the constant phase relationship between arrivals, it makes sense to carry out the averaging along the slope of the striations. In the assumption that the channel invariant  $\beta = 1.0$ , it is known that the striations are along straight lines radiating from the point  $f=0$ ,  $r=0$ . Such a technique is illustrated in Figure 5 in which two striations are shown. As the phase variation between any pair of arrivals is maintained at the same value along the striations, it is tempting to presume that the amplitude values of the summed multi-paths are also unchanged along striations. This is not the case, however, as the bandwidth between striations increases with range, but the average frequency spacing of features scales with  $\Delta f_h$  given by Equation (5) and is unchanged with range.

A measure of the extent of range over which averaging may be carried out along the lines of the striations can be seen as related to the ratio of the increase in the bandwidth,  $\Delta f_2$  in the Figure 5, to the minimum spectral width of features in the spectrum, which may be assumed to be of the order of the value  $\Delta f_h$ . In particular, it may be assumed that  $\Delta f_2$  must be less than  $\Delta f_h$ . It may be shown that

$$\Delta f_2 = (r_2 - r_1)(f_2 - f_1)/r_1. \quad (10)$$

If the slopes of the striations are now assumed to be not greatly different, and if the range and frequency extents  $r_2 - r_1$  and  $f_2 - f_1$  are not large relative to absolute values, it is possible to make some substitutions by use of the expression  $\Delta f/\Delta r = f/r$ . In particular, it may be assumed that  $(r_2 - r_1)/(f_2 - f_1) \approx r_2/f_2 \approx r_1/f_1 \approx r/f$ , and  $f(r_2 - r_1)/r$  may be substituted for  $f_2 - f_1$  in Equation (10), to give

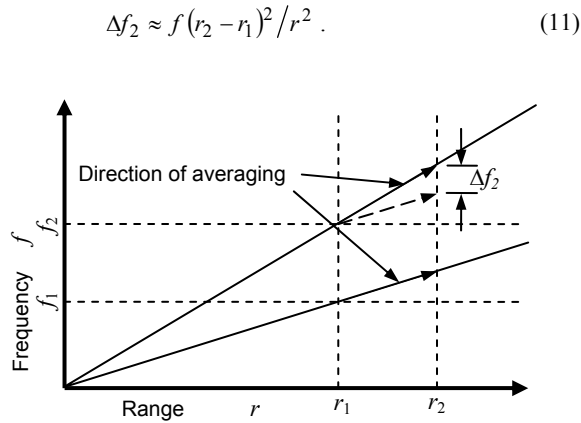


**Figure 5.** Striations on range-frequency plot and implications for averaging spectrum

Requiring  $\Delta f_2$  from Equation (11) to be less than  $\Delta f_h$  from Equation (5) results in the requirement

$$\Delta r = (r_2 - r_1) < r \sqrt{0.037 c_w F / (D f)}. \quad (12)$$

For the previous example (ocean 80 m deep, range 3000 m, frequency 200 Hz), the averaging along the striations must be confined to a range span of  $\Delta r < 180\sqrt{F}$  metres. This is clearly greater than the range span of  $10.4 F$  metres, which was derived earlier when the averaging was confined to fixed frequencies. It is obvious from the pattern of data in Figure 1 that a regime of averaging along lines of constant frequency will not be as successful as averaging along the lines of striations radiating from the point  $f=0, r=0$ . It may be anticipated that striations-based averaging is tolerant to exceedance of the range given by Equation (12), as some of the features will be persistent, while new features are added, and features are removed. For the example considered above, using the value  $F=9$  dB/radian for coarse sand gives a maximum range span for averaging at around 200 Hz  $\Delta r < 600$  metres.

The authors have applied the term “matched slope averaging” to this method of striation-based averaging, and its application to at-sea data is demonstrated in the paper by Clarke and Jones (2012).

### Limitations of Spectral Variability Technique

As outlined by Jones and Clarke (2010) the use of the spectral variability technique is not without limitations. One of these is that the transmission environment must be highly multi-path, or highly multi-modal, in which case the  $TL$  may be expected to not undergo abrupt changes when an extra mode is cut-on or off. It may be speculated that of the order of 5 to 10 modes is required. The frequencies corresponding with cutoff of modes in an isovelocity ocean may be shown to be as follows, from e.g. equation (5.5.9) of Brekhovskikh and Lysanov (2003)

$$f_m = \frac{c_w(m - \frac{1}{2})}{2D\sqrt{1 - (c_w/c_b)^2}} \quad (13)$$

where  $m$  is (integer) number of mode ( $m = 1, 2, 3, \dots$ ),  $c_b$  is the compressional speed of sound in the seafloor, m/s. For the

example of coarse sand,  $c_b = 1800$  m/s, for an ocean of depth 80 m, the cutoff frequency for mode 1 is 8.5 Hz, for mode 2 is 25.4 Hz and for mode 3 is 42.4 Hz. From the low-frequency detail of the  $TL$  data for coarse sand, shown in Figure 6, it is noteworthy that each of these frequencies corresponds with a distinct change in the  $TL$  values at a given range, and is indicative of the need for more modes to be present before “multi-modal” transmission occurs. In the case of coarse sand, for the 80 m deep ocean it appears that 5 modes may be enough (cutoff frequency 76 Hz), and 10 modes (cutoff frequency 161 Hz) is quite adequate.

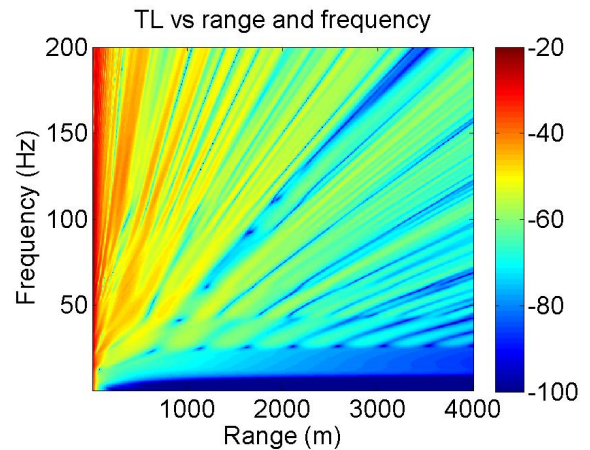


**Figure 6.** Simulated range-frequency  $TL$ , frequency to 200 Hz, for 80 m ocean, coarse sand seafloor

A second requirement is that the transmission range is such that the impulse decay function is known to be dominated by the ocean boundary losses at the seafloor. In such cases the decay function is approximately exponential, and of the form  $e^{-t/\tau}$ . Although not explained here (it is intended to publish full details elsewhere), this imposes an approximate requirement that source to receiver range  $r$  be such that

$$r < 12.6 F D \text{ m}. \quad (14)$$

The essence of this requirement, as described by Equation (14), is that the ocean boundary losses should dominate the impulse decay at, approximately, the time  $4\tau$ , where  $\tau$  is the time for the impulse to decay by  $1/e$ . For the example of the coarse sand seafloor, for an ocean of depth 80 m, the requirement becomes  $r < 9,070$  m.

Lastly, there is a requirement that the angles of incidence at the seafloor of significant multi-paths must be small, so that the interference field is dominated by bottom loss effects in the low angle region for which the variation of bottom loss with grazing angle is approximately linear. If the significant multi-path arrivals are presumed to be received within the time  $4\tau$  of the channel impulse decay function, although not explained here it may be shown that they will be confined to grazing angles less than  $\beta_n \approx 4\sqrt{5D \log(e)/(rF)}$  radians. Assuming that the linear function of bottom loss with grazing angle  $F\beta$  dB will fail for angles exceeding a limiting angle  $\beta_l$ , a source-to-receiver range requirement may be presumed as that for which arrivals received up to time  $4\tau$  in the impulse decay function are at grazing angles less than  $\beta_l$ , such that

$$r > 80 \log_{10}(e) D / (F \beta_i^2) \text{ m}. \quad (15)$$

From the data in Figure 3, for a coarse sand seafloor the limiting grazing angle  $\beta_i$  is, very approximately, about  $17^\circ$  so that this requirement becomes

$$r > 400 D / F \text{ m}. \quad (16)$$

For an ocean of depth 80 m, and a value of bottom loss vs. grazing angle function  $F \approx 9$ , the requirement becomes  $r > 3,500$  m.

Each of the range requirements Equations (14) and (16) becomes problematical for very low values of bottom loss versus grazing angle function  $F$  dB/radian, so the particular case of coarse sand, with its value  $F = 9$  dB/radian is a challenge for the technique.

## DEMONSTRATION OF TECHNIQUE

The striations-based, or matched-slope, averaging technique has been used to invert seafloor reflectivity, as the bottom loss versus grazing angle function  $F$  dB/radian, for simulated data for several seafloor types. An example of this data is presented below. Here, the process has been carried with reference to the frequency limitations of Equation (13) and to the source to receiver range requirements of Equations (14) and (16). Also, the matched slope averaging has been used to obtain a segment of the spectrum of received signal by averaging range-frequency data over a span of ranges appropriate to Equation (12). For these simulations, the range-frequency data were as for a temporally uncorrelated Gaussian signal source. The resultant spectrum was processed to obtain a value of  $F$  as described earlier. Here, the spectral data are processed to obtain the autocorrelation (Equation (9)), the value  $\Delta f_h$ , the frequency displacement at which the autocorrelation of received amplitude with frequency reduces to 0.5, is read off, and  $F$  obtained using Equation (8).

### Data from Coherent Source

To illustrate that the spectral variability technique yields a reasonable estimate of the required bottom loss versus grazing angle value  $F$ , the data in Figure 1 were first processed “as is”. As the data simulates a coherent source at each frequency, no averaging with range is required and none was used. Here the spectrum of data over the band 75 Hz to 500 Hz at each range value was used to obtain a value  $\Delta f_h$ , and  $F$  was obtained by application of Equation (8). The lower limit of 75 Hz was chosen as this corresponded with the cut-on of the 5<sup>th</sup> mode, as mentioned earlier. The derived values of  $\Delta f_h$  are shown in Figure 7. In the region of range values greater than the range minimum of about 3,500 m, the values of  $\Delta f_h$  fluctuate between about 3 and 5 Hz. From Equation (8), this results in values of  $F$  between 4.4 dB/radian and 7.3 dB/radian. These may be seen as reasonable estimates of the true value of 9 dB/radian for the gradient of bottom loss versus grazing angle for small angles. (Note that much larger values of  $F$  apply to absorptive seafloors, e.g.  $F \approx 37$  dB/radian for clay-silt (Jones and Clarke 2010),  $F \approx 60$  dB/radian at 100 Hz for a layered seafloor with a limestone basement (Jones et al. 2008).) They are also in accord with the expectation, mentioned earlier, that  $\Delta f_h$  is about  $1/3^{\text{rd}}$  the spacing between adjacent maxima seen in the data versus frequency in Figure 1 at each range step. It may

be noted that for ranges smaller than the value 3,500 m obtained from Equation (16), multi-path arrivals at grazing angles in excess the desired minimum will become significant. From Figure 3, the bottom loss values for arrivals at angles greater than about  $18^\circ$  are significantly less than if the bottom loss adhered to the assumed function  $F \beta$  dB. The expected effect upon the frequency scale of  $TL$  is for a reduction in  $\Delta f_h$  from that expected at longer ranges – and this appears to be evident in Figure 7. Although not considered further here, it is believed that the local maximum in bottom loss, at just under  $20^\circ$  grazing angle, followed by the large dip in bottom loss near the seafloor critical angle of about  $34^\circ$ , may be attributed to the high shear speed value assumed for coarse sand (600 m/s).

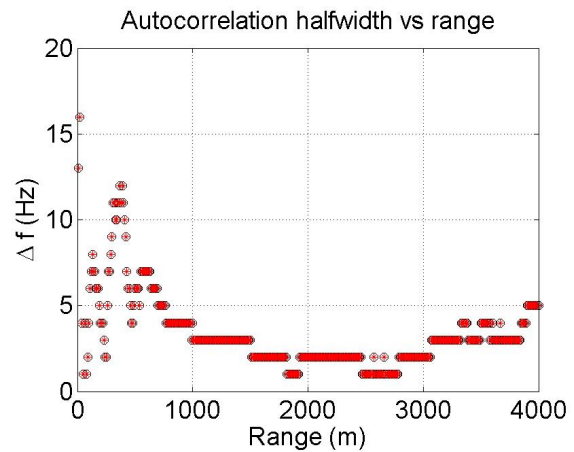
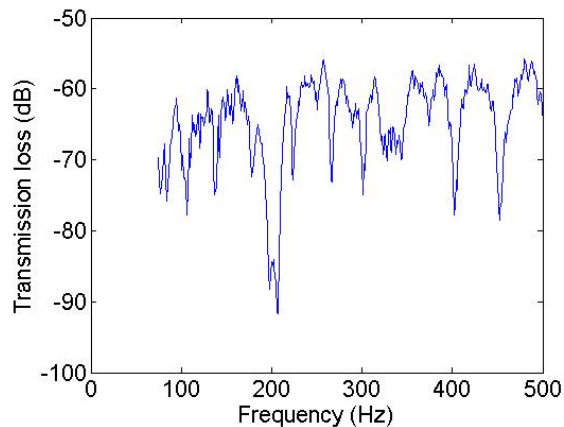


Figure 7. Derived frequency displacement  $\Delta f_h$  as function of range, using data 75 - 500 Hz

### Matched-slope Averaged Data from Incoherent Source

The matched-slope averaging scheme described in this paper was applied to the range-frequency data shown in Figure 4. In accord with the “small angle” minimum range requirement (Equation (16)) and the maximum allowable span of range values (Equation (12)), the matched slope averaging was carried out on data between 75 Hz and 500 Hz, starting at range 3,500 m and concluding at range 4,000 m. Here the frequency span (i.e. 75 – 500 Hz) was determined at the start range (3,500 m).

As the range step for the data in Figure 4 (and in Figure 1) is 10 m, over the 500 m range span there are 50 individual spectra which are to be averaged, using the matched-slope technique. From Equation (7), it is expected that the resulting matched-slope averaged spectrum will have values confined to a scatter of  $\pm 1.2$  dB about the true values of  $TL$  versus frequency, and that the scatter is sufficiently smoothed for the autocorrelation of amplitude values to be carried out in accordance with Equation (9), and a value  $\Delta f_h$  determined. The  $TL$  versus frequency data, obtained using this averaging process, are shown in Figure 8. Note that the frequency scale applied to the data is that taken at the range 3,500 m. Clearly, at 4,000 m the frequency scale will be slightly larger, but this may be ignored with little error in this case.



**Figure 8.** Received level vs. frequency after matched-slope averaging over range 3.5-4.0 km, for 80 m ocean, coarse sand seafloor, uncorrelated Gaussian signal source,  $B\Delta t = 1$

The value of  $\Delta f_h$  obtained from the data in Figure 8 is 7 Hz. By use of Equation (8), we obtain a value for the bottom loss versus grazing angle slope  $F$  of 10.2 dB/radian which is a good fit to the known value of 9 dB/radian. In fact this is a closer estimate than that obtained using the coherent data. The coherent range-frequency  $TL$  data shown in Figure 1 included a few sharp nulls within the 75 Hz to 500 Hz range which were in excess of 20 dB lower than normally expected with Rayleigh distributed data. It is believed that these reduced the  $\Delta f_h$  values obtained from the coherent source data (Figure 7). After matched-slope averaging (see Figure 8), the data from the simulated incoherent source showed that these nulls were not as deep. It is believed that the process of matched-slope averaging resulted in the nulls being “partly filled” as a result of the slight changes in the spectrum which occurred as a function of range.

## CONCLUSIONS

A technique has been presented by which the seafloor reflectivity parameter,  $F$  dB/radian, may be inverted from range-frequency striation data obtained in a shallow ocean environment. The technique is based on the broadband method published previously by the authors, but has been extended to the case of signals received as a function of range. In particular, a method has been presented by which received data may be enhanced, and the inversion accomplished, in the case when the sound source radiates a temporally uncorrelated random Gaussian signal. The method involves averaging along the slope of the striations, and assumes that these are aligned in accordance with a channel invariant  $\beta = 1$ . As with the authors’ previous technique, the inversion is based on the spectral equivalent of the channel impulse response of the shallow water environment, and is achieved through a frequency variability parameter,  $\Delta f_h$  Hz, being the key statistic of spectral variability for the channel. As demonstrated in this paper, the technique is applicable to a seafloor consisting of a uniform half-space, but it is anticipated that some measure of the frequency variation in the seafloor reflectivity parameter  $F$  dB/radian may be extracted by the technique, to a degree suitable for many purposes. As presented here, the technique has limitations in the source to receiver range for which data is suitable, the range span over which the matched-slope averaging may be carried out, and the lower limiting frequency for which data may be processed, however it is considered that these limitations may be managed to useful effect.

## REFERENCES

- Bartel, D. W. 2010, ‘HANKEL: A Tool for Exploring the Complex Pressure Field in Range-Independent Underwater Acoustic Environments’, *Proceedings of 20<sup>th</sup> International Congress on Acoustics, ICA 2010*, Sydney, Australia, 23-27 August
- Blackman, R.B. and Tukey, J.W. 1959, *The measurement of power spectra*, Dover Publications, Inc., New York
- Brekhovskikh, L.M. and Lysanov, Yu.P. 2003, *Fundamentals of Acoustics*, 3<sup>rd</sup> edition, Springer-Verlag, New York
- Clarke, P. A. and Jones, A. D. 2012, ‘Shallow Water Seafloor Inversion using Ship-generated Striations Patterns’, *Proceedings of ACOUSTICS 2012 FREMANTLE*, 21-23 November, Fremantle, Australia
- Heaney, K. D. 2004, ‘Rapid Geoacoustic Characterisation Using a Surface Ship of Opportunity’, *IEEE J. Oceanic Eng.*, vol. 29, no. 1, pp 88 – 99
- Jensen, F. B. and Kuperman, W. A., 1983, ‘Optimum frequency of propagation in shallow water environments’, *J. Acoust. Soc. Am.*, 73, March, pp 813-819
- Jones, A. D., Day, G. J. and Clarke, P. A. 2008, ‘Single parameter description of seafloors for shallow oceans’, *Proceedings of Acoustics '08 Paris*, Paris, France, 29 June – 4 July, pp 1725 – 1730, also published in *Proceedings of the 9<sup>th</sup> European Conference on Underwater Acoustics, ECUA 2008*, Volume 1, pp 161 – 166
- Jones, A. D. and Clarke, P. A. 2010, ‘Rapid seafloor inversion in shallow oceans using broadband acoustic data’, *Proceedings of 20<sup>th</sup> International Congress on Acoustics, ICA 2010*, Sydney, Australia, 23-27 August
- Jones, A. D. and Clarke, P. A. 2011, ‘Seafloor Inversion for Shallow Oceans Using Broadband Acoustic Data’, *Proceedings of 4th International Conference and Exhibition on Underwater Acoustic Measurements: Technologies & Results*, Kos, Greece, 20-24 June, pp 9 – 14
- Schroeder, M. R. 1962, ‘Frequency-Correlation Functions of Frequency Responses in Rooms’, *J. Acoust. Soc. Am.*, 34, No. 12, pp 1819-1823
- Schroeder, M. R. and Kuttruff, K. H. 1962, ‘On Frequency Response Curves in Rooms. Comparison of Experimental, Theoretical and Monte Carlo Results for the Average Frequency Spacing Between Maxima’, *J. Acoust. Soc. Am.*, vol. 34, pp 76 – 80
- Schroeder, M. R. 1987, ‘Statistical Parameters of the Frequency Response Curves of Large Rooms’, *J. Audio Eng. Soc.*, vol. 35, pp 299 – 305
- Urlick, R.J. 1983, *Principles of Underwater Sound*, 3<sup>rd</sup> edition, Peninsula Publishing, Los Altos